

# ANGULAR DOSE VARIATIONS FROM 4- TO 6-MV ROD-PINCH DIODE EXPERIMENTS ON THE ASTERIX PULSED-POWER GENERATOR\*

S.B. Swanekamp<sup>a,b</sup>, R.J. Allen, R.J. Comisso, G. Cooperstein, D. Mosher, and F.C. Young<sup>a</sup>  
*Naval Research Laboratory, Plasma Physics Division, Washington, DC 20375*

C. Vermare, J. Delvaux, Y. Hordé, E. Merle, R. Nicolas, D. Noré, O. Pierret, Y.R. Rosol,  
Y. Tailleur, and L. Véron  
*Polygone d'Expérimentation de Moronvilliers, Moronvilliers, France*

F. Bayol, A. Garrigues, C. Delbos, and G. Nicot  
*Centre d'Etudes de Gramat, Gramat, France*

B.V. Oliver<sup>c</sup>, D.V. Rose<sup>c</sup>, and J. Maenchen  
*Sandia National Laboratories, Albuquerque, NM 87185*

## Abstract

The angular distribution of radiation from a rod-pinch diode is examined with coupled PIC-Monte-Carlo simulations using the LSP code[1] and compared with angular dose measurements on the ASTERIX pulsed-power generator. For the 4- to 6-MV voltage range accessible in the experiments, both the measured and simulated doses at 1 m were 25 to 38 rad-LiF in the forward direction ( $0^\circ$ ). The calculated dose at  $90^\circ$  is 1.2-1.8 times larger than the forward-directed dose depending on both the voltage and rod diameter. This is also in agreement with the measured angular variation[2]. At 6 MV, the simulations show that the dose near  $180^\circ$  is more than twice the forward-directed dose. At these high voltages, electrons approach the anode rod primarily at angles close to  $180^\circ$  resulting in peak radiation in the backward direction. This suggests that negative polarity should be considered for voltages at or above 6 MV to maximize the extracted dose. Simulations show that the  $0^\circ$  dose is higher with tapered rods and increases with rod diameter. Simulations at 10 MV show that the dose near  $180^\circ$  is more than ten times higher than the  $0^\circ$  dose. At 10 MV, the dose near  $180^\circ$  at 1 m from a 2-mm diameter, blunt rod is calculated to be  $\sim 800$  Rad (LiF).

## I. RADIATION MEASUREMENTS AND CALCULATIONS

A standard rod-pinch diode consists of a blunt or tapered tungsten or gold anode rod that protrudes a few cm beyond an annular cathode as shown in Fig. 1. For the Asterix experiments[2,3] analyzed here, the anode was

either a 1- or 2-mm diameter tungsten or gold rod that extended 1.6 cm beyond the cathode annulus and was tapered to a point over the last 1.0 cm. The electron positions from a particle-in-cell (PIC) simulation (see Fig. 1) show that, because of the strong self-magnetic field and the emission of protons from the anode (not shown), electrons are strongly focused onto the tip of a high-atomic-number anode rod. The result is an intense source of x-rays with a source diameter comparable to the diameter of the rod when viewed along the rod axis.[4]

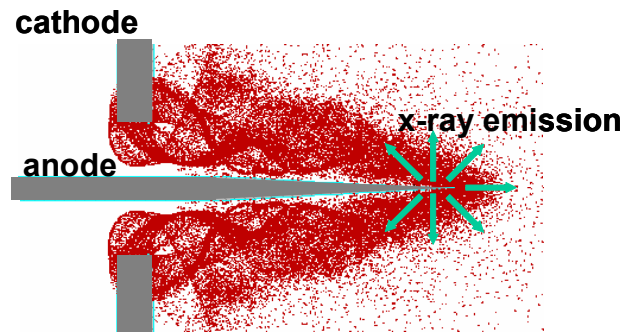


**Figure 1.** Geometry of the rod-pinch diode with electron positions from a PIC simulation.

The angular distribution of the dose is measured at several angles using both thermoluminescent dosimeters (TLDs) and Si *pin* diodes. Time histories of the radiation are measured with an array of six lead-collimated Si *pin* diode detectors. The angular locations of the detectors are shown in Fig. 2. These radiation diagnostics are described in detail in Ref. 2. The tip of the rod is positioned near the center of a 10-cm-radius, 1-cm-thick, hemispherical aluminum shell so that all radiation measurements are attenuated through 1 cm of aluminum.

\* Work supported by the Commissariat a l' Energie Atomique/DAM, Centred' Etudes de Gramat/DGA, and US Department of Energy through Sandia National Laboratories.

<sup>a</sup> Titan/Jaycor, McLean, VA 22102

<sup>b</sup> Email: swane@calvin.nrl.navy.mil

<sup>c</sup> Mission Research Corporation, Albuquerque, NM 87110

## Report Documentation Page

*Form Approved*  
OMB No. 0704-0188

Public reporting burden for the collection of information is estimated to average 1 hour per response, including the time for reviewing instructions, searching existing data sources, gathering and maintaining the data needed, and completing and reviewing the collection of information. Send comments regarding this burden estimate or any other aspect of this collection of information, including suggestions for reducing this burden, to Washington Headquarters Services, Directorate for Information Operations and Reports, 1215 Jefferson Davis Highway, Suite 1204, Arlington VA 22202-4302. Respondents should be aware that notwithstanding any other provision of law, no person shall be subject to a penalty for failing to comply with a collection of information if it does not display a currently valid OMB control number.

1. REPORT DATE <b>JUN 2003</b>	2. REPORT TYPE <b>N/A</b>	3. DATES COVERED <b>-</b>	
4. TITLE AND SUBTITLE <b>Angular Dose Variations From 4- To 6-Mv Rod-Pinch Diode Experiments On The Asterix Pulsed-Power Generator</b>		5a. CONTRACT NUMBER	
		5b. GRANT NUMBER	
		5c. PROGRAM ELEMENT NUMBER	
6. AUTHOR(S)		5d. PROJECT NUMBER	
		5e. TASK NUMBER	
		5f. WORK UNIT NUMBER	
7. PERFORMING ORGANIZATION NAME(S) AND ADDRESS(ES) <b>Naval Research Laboratory, Plasma Physics Division, Washington, DC 20375</b>		8. PERFORMING ORGANIZATION REPORT NUMBER	
9. SPONSORING/MONITORING AGENCY NAME(S) AND ADDRESS(ES)		10. SPONSOR/MONITOR'S ACRONYM(S)	
		11. SPONSOR/MONITOR'S REPORT NUMBER(S)	
12. DISTRIBUTION/AVAILABILITY STATEMENT <b>Approved for public release, distribution unlimited</b>			
13. SUPPLEMENTARY NOTES <b>See also ADM002371. 2013 IEEE Pulsed Power Conference, Digest of Technical Papers 1976-2013, and Abstracts of the 2013 IEEE International Conference on Plasma Science. IEEE International Pulsed Power Conference (19th). Held in San Francisco, CA on 16-21 June 2013. U.S. Government or Federal Purpose Rights License, The original document contains color images.</b>			
14. ABSTRACT <b>The angular distribution of radiation from a rod-pinch diode is examined with coupled PIC-Monte-Carlo simulations using the LSP code[1] and compared with angular dose measurements on the ASTERIX pulsedpower generator. For the 4- to 6-MV voltage range accessible in the experiments, both the measured and simulated doses at 1 m were 25 to 38 rad-LiF in the forward direction (0o). The calculated dose at 90o is 1.2- 1.8 times larger than the forward-directed dose depending on both the voltage and rod diameter. This is also in agreement with the measured angular variation[2]. At 6 MV, the simulations show that the dose near 180o is more than twice the forward-directed dose. At these high voltages, electrons approach the anode rod primarily at angles close to 180o resulting in peak radiation in the backward direction. This suggests that negative polarity should be considered for voltages at or above 6 MV to maximize the extracted dose. Simulations show that the 0o dose is higher with tapered rods and increases with rod diameter. Simulations at 10 MV show that the dose near 180o is more than ten times higher than the 0o dose. At 10 MV, the dose near 180o at 1 m from a 2-mm diameter, blunt rod is calculated to be ~800 Rad (LiF).</b>			
15. SUBJECT TERMS			
16. SECURITY CLASSIFICATION OF:			17. LIMITATION OF ABSTRACT
a. REPORT <b>unclassified</b>	b. ABSTRACT <b>unclassified</b>	c. THIS PAGE <b>unclassified</b>	<b>SAR</b>
			18. NUMBER OF PAGES <b>4</b>
			19a. NAME OF RESPONSIBLE PERSON



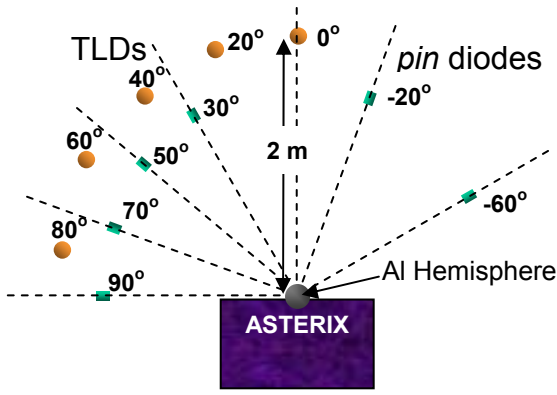


**Figure 2.** A schematic illustrating the positions of the radiation diagnostics used in the Asterix experiments.

The measurements show that the dose increases with angle and the *pin* diodes at large angles are subject to saturation effects.[2] Therefore, the pulse-shape from the *pin* diode located at  $-20^\circ$  is used to compare the measured and calculated dose-rates. There is no evidence of saturation effects in the smaller signals from this detector. The time-histories of the radiation at the various TLD locations is then inferred by scaling the  $-20^\circ$  *pin* diode pulse-shape so that the time-integral is the TLD dose at that location. This scaling is appropriate because the measured TLD doses were observed to scale linearly with the dose from the *pin* diodes in a previous experiment on Asterix.

The angular distribution of the radiation from a rod-pinch diode is calculated with the particle-in-cell (PIC) code, LSP[1,5]. LSP incorporates electron scattering, energy loss, and bremsstrahlung production algorithms from the Integrated Tiger Series[6] (ITS) of electron-photon Monte-Carlo transport codes. The method which is used to calculate the angular dose distribution is similar to that used to calculate the forward-directed ( $0^\circ$ ) dose for voltages up to 4 MV.[5] First, LSP is run to steady state for a number of voltages. Once a steady-state voltage is achieved, a list of electron positions and momenta incident on the surface of the rod is generated. The electron list is post-processed with the ITS code, CYLTRAN, to calculate the angular distribution of the radiation spectrum emerging from the rod. An alternative method of calculating the radiation spectrum utilizes the capability of LSP to generate a list of photons that contains their energy, direction, and location in the rod as they are created. The angular distribution of the radiation spectrum is then calculated by using CYLTRAN to model self-absorption in the rod. This is the method used in Ref. 5. The two methods provide an excellent cross-check and we have found that both methods produce essentially the same results.

The angular-dose distribution at 1 meter is calculated from the radiation spectrum using

$$\frac{Dose(\theta)}{Q_e} = \int_0^\infty R(h\nu)F(h\nu) \frac{d\Phi_s(\theta, h\nu)}{d(h\nu)} d(h\nu), \quad (1)$$

where  $Q_e$  is the incident electron charge on the rod,  $R(h\nu)$  is the spectral response of the detector [dose per photon flux],  $F(h\nu)$  is the attenuation from any filters between the source and the detector, and  $d\Phi_s/d(h\nu)$  is the angular distribution of the photon flux spectrum per incident electron charge calculated from the LSP/CYLTRAN model. Both the detector response and the filter attenuation are calculated using tabulated attenuation/absorption coefficients.[7] This approach avoids the problem of poor photon counting statistics associated with the small solid angle subtended by the detectors incurred with direct modeling of the detectors with ITS. However, Eq. (1) omits radiation scattered in the filters that can subsequently reach the detector and it can overestimate the energy absorbed energy in the detector if it is not properly equilibrated. Both of these effects are small in this experiment and the forward dose predicted by Eq. (1) agrees with that calculated in Ref. 5 where the detectors are modeled directly with ITS.

The incident electron charge on the rod in Eq. (1) must be calculated in terms of measurable quantities to be useful in comparing with experiments. This charge is determined from the measurables as

$$Q_e = Q_T N_{passes} (1 - I_{ion}/I_T), \quad (2)$$

where  $Q_T$  is the total absorbed charge (i.e. the integral of the current) in the diode (both electrons and ions),  $N_{passes}$  is the number of passes the electrons make in the rod defined by the ratio of incident electron charge to absorbed electron charge, and  $I_{ion}/I_T$  is the ion-current fraction.  $N_{passes}$  can be obtained from either CYLTRAN or LSP and, for 1- and 2-mm diameter tapered rods, the simulations show that electrons make between 2 and 10 passes through the rod as the voltage increases from 2 to 10 MV. The ion current fraction from LSP varies from 25% to 45% when protons are the ion species and it is a weak function of the voltage. For blunt rods, electrons make only 2 to 3 passes through the rod and the ion current fraction is reduced to 25% to 35% for voltages between 2 and 10 MV since electrons spend less time in the diode. To apply Eq.(1) to time-dependent experiments, the dose-per-charge is interpreted as the dose-rate divided by the total current so that

$$Dose/Q_T = (Dose-Rate)/I_T, \quad (3)$$

where  $I_T$  is the total current in the diode. This relationship is valid since the LSP calculations are at steady-state.

Results from angular dose calculations for a 2-mm diameter tapered rod are shown in Fig. 3. The calculations show that the angular variation of the dose-rate efficiency ( $Dose-Rate/I_T$ ) is small for voltages below 4 MV but increases rapidly above 4 MV. The simulations also show that the  $0^\circ$  dose-rate efficiency becomes insensitive to changes in the voltage for voltages above 6 MV. This insensitivity is due to electron angles of incidence on the rod approaching  $180^\circ$  as the voltage increases which increases the x-ray emission at large angles increases relative to the smaller angles. The model predicts that the dose-rate efficiency at 6 MV is

more than a factor of 2 higher near  $180^\circ$  than at  $0^\circ$  (dose at exactly  $180^\circ$  decreases due to self-absorption in the rod). This suggests that, to maximize the extracted dose, future rod-pinch diode experiments at or above 6 MV should be performed in negative polarity with an appropriately designed anode to minimize self-absorption.[8] Also shown in Fig. 3 are power-law fits to the dose-rate at various angles of the form  $A I V^m$ . These fits apply to voltages up to 6 MV and are used to model the Asterix experiments where peak voltages ranged between 4- and 6-MV.

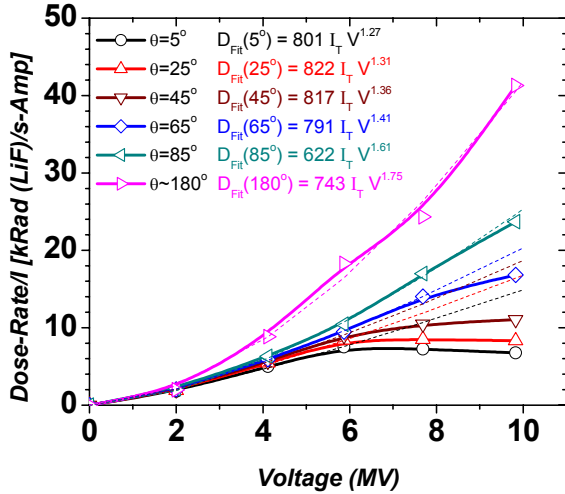


**Figure 3.** Dependence of the dose-rate efficiency on voltage for various angles. Open symbols are from simulations and dashed lines are power-law fits for voltages up to 6 MV.

Calculated and measured dose-rates for a typical Asterix shot are compared in Fig. 4. The calculated dose-rates are obtained using the measured current and voltage waveforms (shown in Fig. 4A) in the power-law fits from the simulations. The diode voltage is obtained by applying a rather large inductive correction ( $L=1030$  nH) to an electrolytic resistive divider located upstream of the diode.[3] As a result, there is a rather large uncertainty in the voltage waveform. The current is an average of three B-dot loops located near the diode load. The variation of the individual B-dots from this average is small indicating a less than  $\pm 5\%$  uncertainty on the current. The magnitudes and shapes of the dose-rates calculated from the LSP/CYLTRAN model are compared with the measured dose-rates at  $0^\circ$ ,  $20^\circ$ ,  $40^\circ$ ,  $60^\circ$ , and  $80^\circ$  in Figs. 4B-4F. A comparison of the angular variation of the total calculated dose (i.e. the time-integral of the dose-rate) and measured the measured TLD dose are shown in Fig. 5. The calculated doses and dose-rates are in agreement with the measurements to within the experimental precision. Similar agreement is obtained for a shot that used 1-mm diameter tapered tungsten rod.

A comparison of the calculated dose-rate efficiencies from 1-mm (Fig. 6A) and 2-mm (Fig. 6B) diameter tapered and blunt rods are shown in Fig. 6. For a given rod diameter, this figure shows that the  $0^\circ$  dose-rate

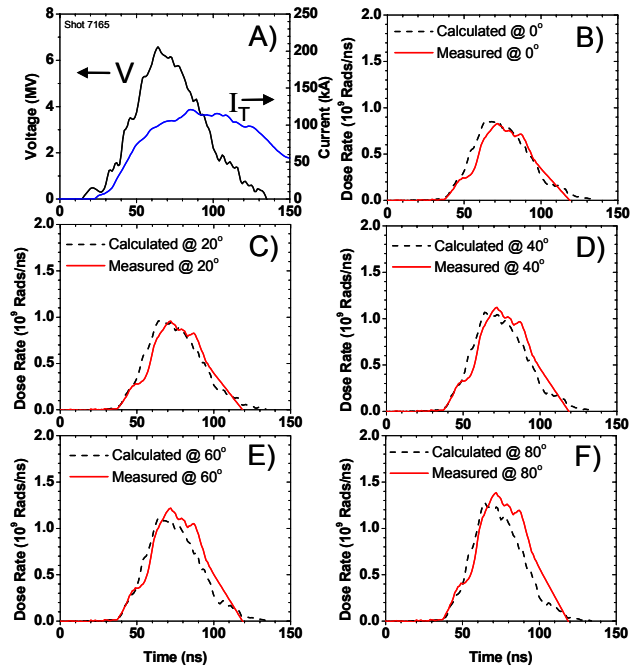


**Figure 4.** Comparison of measured dose-rates with calculated dose-rates for a 2-mm diameter, tapered tungsten rod. A) The voltage and current waveforms. B)  $0^\circ$  dose-rates. C)  $20^\circ$  dose-rates. D)  $40^\circ$  dose-rates. E)  $60^\circ$  dose-rates. F)  $80^\circ$  dose-rates.

efficiency is higher for tapered rods than blunt rods. Near  $180^\circ$ , the dose-rate efficiency from blunt rods is significantly higher than the tapered rods. The dose-rate efficiency at 10 MV is also seen to be more than ten times higher near  $180^\circ$  than at  $0^\circ$ . This suggests that blunt rods are better able to take advantage of the electron angles of incidence as the voltage increases. The calculations at 10 MV indicate a current of  $I_T=210$  kA for a ratio of the cathode-to-anode radii of  $r_C/r_A=11$ . Therefore, a dose of  $\sim 800$  Rad (LiF) near  $180^\circ$  is possible 1 m from a 2-mm diameter, blunt rod in a 50-ns full-width at half maximum radiation pulse. Further increases in the dose are possible if the ion current fraction ( $\sim 40\%$  at 10 MV) can be

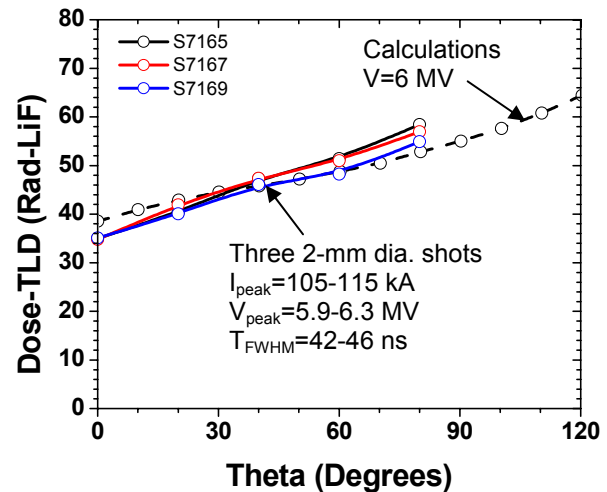


**Figure 5.** Comparison of calculated and measured angular dose variation for a 2-mm diameter, tapered tungsten rod.

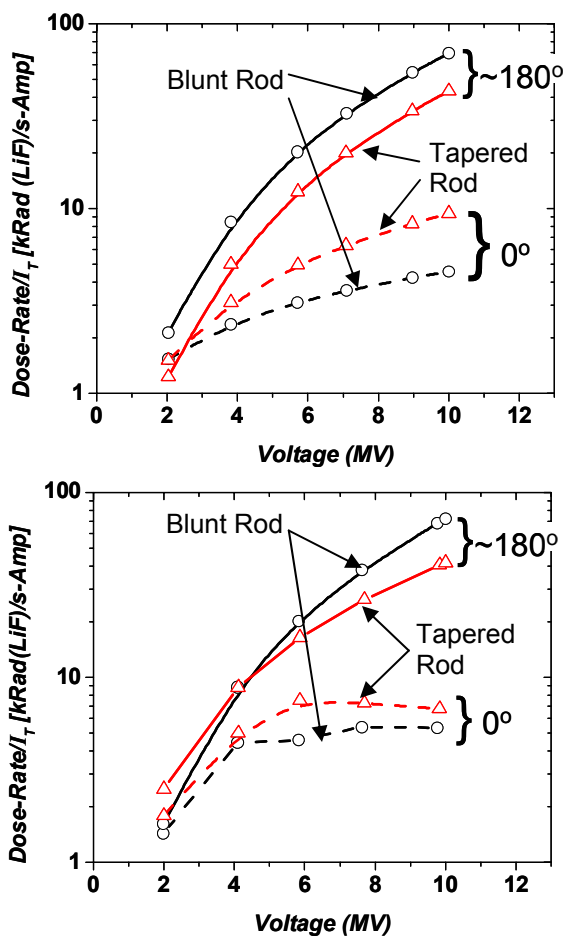


**Figure 6.** Comparison of the calculated  $0^\circ$  and  $180^\circ$  dose-rate efficiencies for blunt and tapered rods. A) 1-mm diameter rods. B) 2-mm diameter rods.

reduced by eliminating protons. When protons are replaced by tungsten ions, the ion current fraction is reduced to less than 5% and the dose increases by 50%. One method for eliminating protons is to heat the tungsten anode to about 2000° K prior to the shot to drive off impurities.[9]

The simulations indicate very little difference in the dose-rate efficiency from 1- and 2-mm diameter blunt rods at  $180^\circ$ . This can be understood by comparing the current flow patterns from 1- and 2-mm diameter blunt rod pinch diodes at 10 MV shown in Fig. 7. From this figure it is seen that electrons  $\mathbf{E} \times \mathbf{B}$  drift down the length of the rod along the virtual cathode surface defined by  $|\mathbf{E}| \sim 0$ . The strong self-magnetic field causes the current flow to bend around the end of the rod and the majority of the current flow enters the rod perpendicular to the end of the rod for both the 1-mm diameter (Fig. 7A) and the 2-mm diameter (Fig. 7B) blunt rods. In both cases the majority of the electron beam couples to the rod axially and not radially so that the x-ray production efficiency is independent of the rod diameter. Side viewing x-ray images indicate that a significant fraction of the electrons are concentrated at the end of the blunt rod.[10]

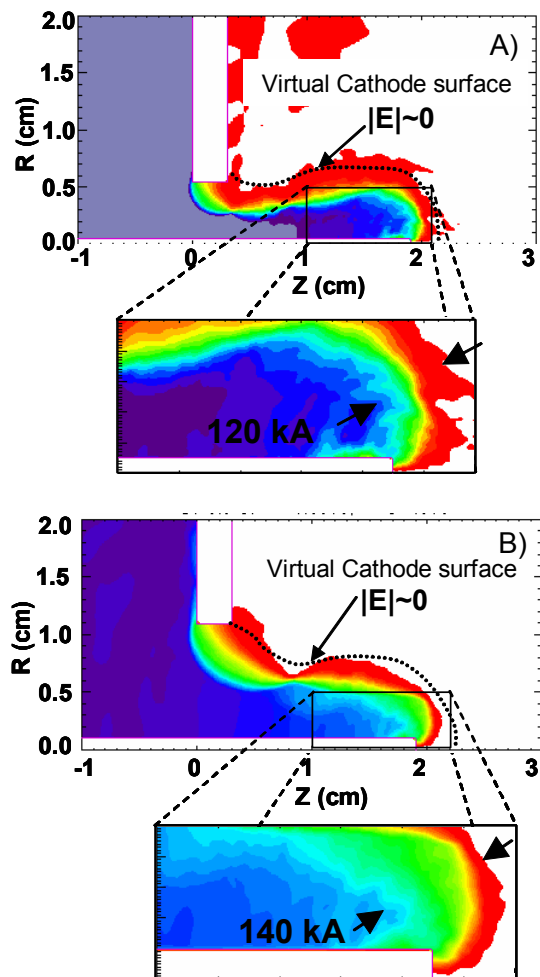


**Figure 7.** Current flow patterns from LSP simulations of a 10 MV, blunt-anode, rod-pinch diode with  $r_C/r_A=11$ . A) 1-mm diameter rod. B) 2-mm diameter rod.

## REFERENCES

- [1] D.R. Welch, D.V. Rose, B.V. Oliver, and R.E. Clark, Nucl. Meth. Phys. Res. A **464**, 134 (2001).
- [2] F.C. Young, et al., these proceedings.
- [3] R.J. Commisso, et al., these proceedings.
- [4] R.J. Commisso, D.D. Hinshelwood, D. Mosher, P.F. Ottinger, S.J. Stephanakis, S.B. Swanekamp, B.V. Weber, and F.C. Young, IEEE Trans. Plas. Sci. **30**, 338 (2002).
- [5] D.V. Rose, D.R. Welch, B.V. Oliver, R.E. Clark, D.L. Johnson, J.E. Maenchen, P.R. Menge, C.L. Olson, and D.C. Rovang, J. Appl. Phys. **91**, 3328 (2002).
- [6] J.A. Halbleib, R.P. Kensek, G.D. Valdez, S.M. Seltzer, and M.J. Berger, IEEE Trans. Nucl. Sci. **41**, 1025 (1992).
- [7] NIST tables are available online at <http://physics.nist.gov/PhysRefData/XrayMassCoef>.
- [8] G. Cooperstein, et al., these proceedings.
- [9] B. V. Weber, R. J. Allen, B. G. Moosman, S. J. Stephanakis, F. C. Young, N. R. Pereira, J. R. Goyer, IEEE Trans. Plasma Sci., **30**, 1806 (2002).
- [10] D. Mosher et al., these proceedings.